



Circuit approach to photonic heat transport

Laëtitia Pascal, Hervé Courtois, Frank. W. J. Hekking

► To cite this version:

Laëtitia Pascal, Hervé Courtois, Frank. W. J. Hekking. Circuit approach to photonic heat transport. *Physical Review B: Condensed Matter and Materials Physics (1998-2015)*, 2011, 83 (12), pp.125113. 10.1103/PhysRevB.83.125113 . hal-00520909

HAL Id: hal-00520909

<https://hal.science/hal-00520909v1>

Submitted on 16 Mar 2022

HAL is a multi-disciplinary open access archive for the deposit and dissemination of scientific research documents, whether they are published or not. The documents may come from teaching and research institutions in France or abroad, or from public or private research centers.

L'archive ouverte pluridisciplinaire **HAL**, est destinée au dépôt et à la diffusion de documents scientifiques de niveau recherche, publiés ou non, émanant des établissements d'enseignement et de recherche français ou étrangers, des laboratoires publics ou privés.

Circuit approach to photonic heat transport

L. Pascal¹, H. Courtois¹ and F. W. J. Hekking²

¹*Institut Néel, CNRS and Université Joseph Fourier,*

25 Avenue des Martyrs, BP 166, 38042 Grenoble, France.

²*LPMMC, Université Joseph Fourier and CNRS,*

25 Avenue des Martyrs, BP 166, 38042 Grenoble, France.

(Dated: October 30, 2018)

We discuss the heat transfer by photons between two metals coupled by a circuit containing linear reactive impedances. Using a simple circuit approach, we calculate the spectral power transmitted from one metal to the other and find that it is determined by a photon transmission coefficient, which depends on the impedances of the metals and of the coupling circuit. We study the total photonic power flow for different coupling impedances, both in the linear regime, where the temperature difference between the metals is small, and in the non-linear regime of large temperature differences.

PACS numbers: 65.80.-g, 44.40.+a

I. INTRODUCTION

Electron thermodynamics at the nano-scale is a fast developing topic,¹ in particular in superconductor-based hybrid devices. For instance, Superconductor-Insulator-Normal (S-I-N) metal junctions biased just below the superconducting energy gap display electronic cooling.^{1,2} The thermal properties of S-N and S-N-S hybrid devices also show signatures of quantum phase coherence.³

In metallic systems, heat conduction can be achieved by electrons, phonons and also photons.^{4,5} The photonic channel was recently revealed experimentally^{6,7} at very low temperature in devices including superconducting transmission lines. In a superconductor, electrons are paired into Cooper pairs so that the electron-phonon coupling is vanishing,⁸ just as the electronic heat conductance. Therefore, only photons can contribute to the heat transfer at very low temperature. With a good matching between the source and the drain, the conductance of a superconducting transmission line is equal to the thermal conductance quantum:⁹ $K_Q = k_B^2 T \pi / 6\hbar$.

The photonic channel for heat transfer can in principle couple metallic systems that are galvanically isolated, e.g. through a capacitor. This effect can be beneficial in some cases, but also detrimental when one wants to maintain two electronic populations at different quasi-equilibrium temperatures. An inductance can also be present in some realistic configurations, due to the wiring geometry. In this paper, we investigate the photonic heat transfer through a general reactive impedance, i.e. a linear coupling circuit that contains a capacitor, an inductance, a resonant circuit or a transmission line. We follow a simple circuit approach, valid at low temperatures when the relevant photons have wavelengths larger than the size of the typical circuit element. The metallic parts can then be treated as lumped elements characterized by an electrical impedance. We present a quantitative analysis, enabling us to establish design rules for useful devices, including phonon thermometers or electron coolers.

II. CIRCUIT APPROACH

We consider the circuits A, B and C shown in Fig. 1. These configurations contain two impedances $Z_i(\omega)$ ($i = 1, 2$), kept at different temperatures T_i such that $T_2 > T_1$. We wish to analyze heat flow between these elements driven by the temperature difference only, i.e. in the absence of any voltage or current source. In configurations A and C, the two impedances belong to *the same* circuit and are coupled through a purely reactive coupling element with impedance $Z_c(\omega)$ or a transmission line. Configuration A is a generalization of the one considered in Ref. 5. In configuration B, the two impedances belong to *two different* circuits, both coupled via a mutual inductance M to a third linear circuit that mediates the heat transfer. Again we assume this coupling circuit to contain reactive elements only with a total impedance $Z_c(\omega)$. Configuration B was analyzed in Ref. 10 with non-equilibrium Green function techniques; here we will show that our circuit approach yields the same results. To the best of our knowledge, configuration C has not been analyzed until now.

In the absence of voltage or current sources, electromagnetic fluctuations are responsible for the heat flow between impedances. We therefore start our analysis by analyzing the current and voltage fluctuations induced by the various circuit elements. Following Ref. 11, we decompose the fluctuating current ΔI_i through the i th element into two parts:

$$\Delta I_i = \delta I_i + (1/Z_i)\Delta V_i. \quad (1)$$

The quantity ΔV_i is the voltage fluctuation across the element i . The fluctuation δI_i is the intrinsic fluctuation produced by the element due to Johnson-Nyquist noise with spectral function

$$\langle \delta I_i(\omega) \delta I_i(\omega') \rangle = 2\pi\delta(\omega + \omega')C_i^{(2)} \quad (2)$$

where $\langle \dots \rangle$ denotes a thermal average and

$$C_i^{(2)} = \hbar\omega \text{Re}[1/Z_i(\omega)] \coth(\frac{\beta_i \hbar\omega}{2}), \quad (3)$$

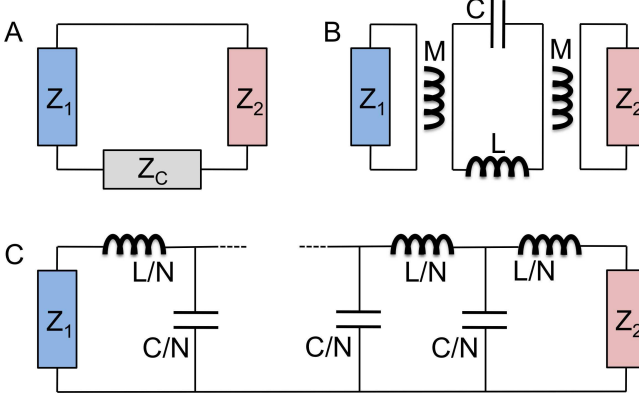


FIG. 1: Top left panel, circuit A: two impedances Z_1 and Z_2 are coupled by a purely reactive coupling impedance Z_c . Top right panel, circuit B: two impedances Z_1 and Z_2 are coupled via mutual inductances to a purely reactive central circuit of total impedance Z_c (here an LC resonator). Bottom panel, circuit C: two impedances Z_1 and Z_2 are coupled via a transmission line.

with $\beta_i = 1/k_B T_i$ being the inverse temperature of element i . The δ -function in Eq. (2) reflects the fact that we consider noise in the stationary limit; Eq. (3) is the fluctuation-dissipation theorem,¹² written in a form appropriate for Johnson-Nyquist noise generated by an impedance Z_i , kept at an inverse temperature β_i .

Certain constraints apply to the fluctuations ΔI_i and ΔV_i . For instance in circuit A, current conservation implies $\Delta I_i = \Delta I_j \equiv \Delta I$ for any element $i, j = 1, 2, c$; similarly, $\sum_i \Delta V_i = 0$. We assume these constraints to be satisfied simultaneously for each element; this implies that we consider fluctuations at low frequencies ω such that the wavelengths $\lambda_\omega \propto 1/\omega$ of the relevant electromagnetic waves are larger than the typical size of the circuit. At 1 Kelvin, this corresponds to a maximum circuit size of about 1 cm; this limit scales as $1/T$.

We will be interested in the net power $P_i(t)$ absorbed by the element $i = 1, 2$ as a function of the temperature difference $\Delta T = T_2 - T_1$ between them. This quantity is given by $P_i(t) = \langle \Delta I_i(t) \Delta V_i(t) \rangle$. It can be expressed in terms of the frequency-dependent correlation function $\langle \Delta I_i(\omega) \Delta V_i(\omega') \rangle$:

$$P_i(t) = \int \frac{d\omega}{2\pi} \int \frac{d\omega'}{2\pi} e^{-i\omega t} e^{-i\omega' t} \langle \Delta I_i(\omega) \Delta V_i(\omega') \rangle. \quad (4)$$

We will calculate and analyze this quantity in detail below for circuits A, B and C.

III. CALCULATION OF THE HEAT EXCHANGE

A. Heat exchange with direct coupling

Let us first consider circuit A in Fig. 1, for the simple case where the reactive coupling element is absent,

$Z_c(\omega) = 0$. Imposing the constraints on ΔI_i and ΔV_i , we obtain $\Delta V_1(\omega) = -\Delta V_2(\omega) = Z_1(\omega)Z_2(\omega)[\delta I_2(\omega) - \delta I_1(\omega)]/[Z_1(\omega) + Z_2(\omega)]$. Using Eq. (2) and the fact that the current noise in different elements is uncorrelated, $\langle \delta I_1 \delta I_2 \rangle = 0$, we find after some elementary algebra,

$$\begin{aligned} \langle \Delta I_1(\omega) \Delta V_1(\omega') \rangle &= -\langle \Delta I_2(\omega) \Delta V_2(\omega') \rangle = \\ &2\pi\delta(\omega + \omega') \frac{Z_1(\omega')Z_2(\omega')}{Z_t(\omega)Z_t(\omega')} \\ &\times [Z_2(\omega)C_2^{(2)}(\omega) - Z_1(\omega)C_1^{(2)}(\omega)]. \end{aligned} \quad (5)$$

Here $Z_t(\omega) = Z_1(\omega) + Z_2(\omega)$ is the total series impedance of the two elements. Substituting Eq. (5) into Eq. (4), using Eq. (3) and integrating over ω' , we find

$$P_1(t) = -P_2(t) = \int_{-\infty}^{+\infty} \frac{d\omega}{2\pi} \frac{2\hbar\omega \text{Re}[Z_1(\omega)] \text{Re}[Z_2(\omega)]}{|Z_t(\omega)|^2} [n_2(\omega) - n_1(\omega)], \quad (6)$$

where we made use of the relation $Z(-\omega) = Z^*(\omega)$ as well as of the identity $\coth x = 1 + 2n(x)$, with $n(x) = [e^x - 1]^{-1}$. The result reflects energy conservation: the power emitted by one of the elements is absorbed by the other.

If we define an effective photon transmission coefficient

$$\mathcal{T}(\omega) = \frac{4\text{Re}[Z_1(\omega)]\text{Re}[Z_2(\omega)]}{|Z_t(\omega)|^2}, \quad (7)$$

and use the fact that the integrand is an odd function of ω to restrict the integration to positive frequencies only, we can write:

$$P_1(t) = -P_2(t) = \int_0^{\infty} \frac{d\omega}{2\pi} \hbar\omega \mathcal{T}(\omega) [n_2(\omega) - n_1(\omega)]. \quad (8)$$

Note that this expression is similar to the one used to discuss heat transport in electron¹³ and phonon systems¹⁴ within the scattering approach. The net heat current is obtained as the difference of the two heat-currents emanating from impedances 1 and 2, that serve as photonic reservoirs each characterized by an equilibrium Bose-Einstein distribution function at temperature $T_{1,2}$. Part of the total heat current injected by the photonic reservoirs can be reflected back, due to a mismatch between impedances Z_1 and Z_2 . The amount of back-reflection can be frequency dependent; it is described by the frequency-dependent transmission coefficient $\mathcal{T}(\omega) \leq 1$.

Interestingly, as we will show below, Eqs. (7) and (8) describe the heat transfer between impedances 1 and 2 for arbitrary configurations A, B and C, as long as the coupling elements are purely reactive. The corresponding total impedance Z_t will be a configuration-dependent function of Z_1 , Z_2 and the impedance of the coupling element.

We will be interested in the heat transfer between elements 1 and 2 as a function of the temperature difference

$\Delta T = T_2 - T_1$. For later use we define $\Delta\beta = \beta_1 - \beta_2$ and $\beta = (\beta_1 + \beta_2)/2$; then Eq. (8) can be rewritten as

$$P_1(t) = -P_2(t) = \int_0^\infty \frac{d\omega}{2\pi} \hbar\omega \mathcal{T}(\omega) \frac{\sinh \Delta\beta\hbar\omega/2}{\cosh \beta\hbar\omega - \cosh \Delta\beta\hbar\omega/2}. \quad (9)$$

If the temperature difference $\Delta T = T_2 - T_1$ is small compared to T_1 or T_2 , we can expand the integrand to first order in $\Delta\beta$. The expression (9) then reads

$$P_{1,2}(t) = \pm \int_0^\infty \frac{d\omega}{2\pi} \hbar\omega \mathcal{T}(\omega) \frac{\Delta\beta\hbar\omega/2}{\cosh \beta\hbar\omega - 1}, \quad (10)$$

and can be further simplified to:

$$P_{1,2}(t) = K\Delta T = \frac{T k_B^2}{\pi\hbar} \int_0^\infty dx \mathcal{T}(x) \frac{x^2}{\sinh^2(x)} \Delta T. \quad (11)$$

where $T = (T_1 + T_2)/2$ is the average temperature and K is the thermal conductance.

Furthermore, if the two impedances 1 and 2 are two identical resistances, so that $R_1 = R_2 = R$, the photon transmission coefficient $\mathcal{T} = 1$ and the thermal conductance K is given by its quantized value, $K = K_Q = k_B^2 T \pi / 6\hbar$. For mismatched resistances $R_1 \neq R_2$, the photon transmission coefficient \mathcal{T} is smaller than 1 and the thermal conductance K will be less than K_Q .

B. Heat exchange with reactive coupling

Let us now consider the more general case of circuit A with a non-zero reactive coupling impedance, following the same approach. Since no noise is generated in a purely reactive element, the spectral noise current through it is simply given by

$$\Delta I_c = \Delta V_c / Z_c. \quad (12)$$

Imposing the constraint on ΔI_i we then find $\Delta I(\omega) = [Z_1(\omega)\delta I_1(\omega) + Z_2(\omega)\delta I_2(\omega)]/Z_t(\omega)$. Now $Z_t(\omega)$ includes the coupling impedance, $Z_t(\omega) = Z_1(\omega) + Z_2(\omega) + Z_c(\omega)$. The constraint on ΔV_i leads to $\Delta V_1(\omega) + \Delta V_2(\omega) = -Z_c(\omega)\Delta I(\omega)$. Moreover, $Z_1(\omega)\Delta V_2(\omega) - Z_2(\omega)\Delta V_1(\omega) = Z_1(\omega)Z_2(\omega)[\delta I_1(\omega) - \delta I_2(\omega)]$. This system of equations can be solved for ΔV_1 and ΔV_2 . The purely reactive impedance will neither emit nor absorb any power, we therefore obtain

$$P_1(t) = \langle \Delta I_1 \Delta V_1 \rangle = -\langle \Delta I_2 \Delta V_2 \rangle = -P_2(t). \quad (13)$$

A straightforward calculation then yields Eqs. (7) and (8), with the appropriate re-definition of the total series impedance $Z_t = Z_1 + Z_2 + Z_c$. This result generalizes the one presented in Ref. 6.

C. Heat exchange with mutual inductive coupling

In this subsection, we consider configuration B, see Fig. 1. The mutual inductance M relates the current fluctuations ΔI_c in the central coupling circuit to the voltage fluctuations in the two outer circuits, $\Delta V_{1,2}(\omega) = i\omega M \Delta I_c(\omega)$, hence we have $\Delta I_i(\omega) = \delta I_i(\omega) + i\omega M \Delta I_c(\omega) / Z_i(\omega)$. On the other hand, the current fluctuations ΔI_1 and ΔI_2 in the outer circuits are related to the fluctuation ΔI_c in the central circuit, according to the relation $\Delta I_c(\omega) = i\omega M [\Delta I_1(\omega) + \Delta I_2(\omega)] / Z_c(\omega)$, where $Z_c(\omega)$ is the total series impedance of the elements in the central circuit, which we assume to be entirely reactive. Combining these observations, we conclude that

$$\Delta I_c(\omega) = \frac{i\omega M [\delta I_1(\omega) + \delta I_2(\omega)]}{Z_c(\omega) + \omega^2 M^2 [1/Z_1(\omega_1) + 1/Z_2(\omega_2)]}. \quad (14)$$

We substitute this result into the expressions for $\Delta I_i(\omega)$ and $\Delta V_i(\omega')$, multiply them and obtain the power absorbed by the impedance Z_i upon the appropriate Fourier transformation according to Eq. (4). Using the fact that $Z_c(\omega)$ is purely imaginary, we again find Eqs. (7) and (8) to hold, but with the total impedance given by:

$$Z_t(\omega) = Z_1(\omega) + Z_2(\omega) + Z_c(\omega) \frac{Z_1(\omega)Z_2(\omega)}{\omega^2 M^2}. \quad (15)$$

This is in agreement with the result obtained in Ref. 10. However, we wish to note it is obtained here from quite simple circuit considerations, without the need of a Green function formalism.

D. Heat exchange through a transmission line

Let us finally study case C, see Fig. 1. A transmission line is represented by a series of N cells, each composed by an inductance L/N and a capacitance C/N . Considering again a photon wavelength larger than the size of a typical circuit element, we apply Kirchhoff's law locally and find a recurrence equation between the potential V_n at element n and the ones for the neighboring cells V_{n-1} and V_{n+1} :

$$V_{n-1} + V_{n+1} + \left(\omega^2 \frac{LC}{N^2} - 2 \right) V_n = 0. \quad (16)$$

Writing the local voltage as a plane wave $V_n \propto e^{i(kn - \omega t)}$ we obtain the dispersion relation

$$\cos k = 1 - \frac{\omega^2 LC}{2N^2}, \quad (17)$$

describing propagating waves with a wave-vector dependent group velocity, thus taking into account retardation effects in the line. Writing the expression of the current

at both extremities of the transmission line we find

$$\Delta I_1 = -\frac{\Delta V_1}{Z_A} + \frac{\Delta V_2}{Z_B}, \quad (18)$$

$$\Delta I_2 = -\frac{\Delta V_2}{Z_A} + \frac{\Delta V_1}{Z_B}, \quad (19)$$

with the characteristic line impedances Z_A and Z_B defined as

$$Z_A = \frac{i\omega L}{N(1 - \cos k + \sin k \cot kN)}, \quad (20)$$

$$Z_B = -i\omega \frac{L \sin kN}{N \sin k}. \quad (21)$$

Identifying the above expressions with Eq. (1) enables us to write the voltages V_1 et V_2 at the resistors 1,2 as a function of the intrinsic current fluctuations δI_1 et δI_2 :

$$\Delta V_2 = \frac{Z_B^2 \tilde{Z}_2}{\tilde{Z}_1 \tilde{Z}_2 - Z_B^2} \delta I_2 + \frac{Z_B \tilde{Z}_1 \tilde{Z}_2}{\tilde{Z}_1 \tilde{Z}_2 - Z_B^2} \delta I_1, \quad (22)$$

$$\Delta V_1 = \frac{Z_B^2 \tilde{Z}_1}{\tilde{Z}_1 \tilde{Z}_2 - Z_B^2} \delta I_1 + \frac{Z_B \tilde{Z}_1 \tilde{Z}_2}{\tilde{Z}_1 \tilde{Z}_2 - Z_B^2} \delta I_2, \quad (23)$$

where we have defined

$$\frac{1}{\tilde{Z}_{1,2}} = \frac{1}{Z_{1,2}} + \frac{1}{Z_A}. \quad (24)$$

Using Eq. (4) while writing the quantities $\Delta V_i(\omega)$ and $\Delta I_i(\omega)$ in terms of the current fluctuations δI_i gives the expression of the power absorbed by the impedance Z_i . We again obtain Eqs. (7) and (8) to hold, with the total impedance given by:

$$Z_t(\omega) = i\omega \frac{L \sin kN}{N \sin k} + \frac{\cos k(N - 1/2)}{\cos k/2} [Z_1 + Z_2] + \frac{Z_1 Z_2 N}{i\omega L} \left[\left(\frac{\cos k(N - 1/2)}{\cos k/2} \right)^2 - 1 \right] \frac{\sin k}{\sin kN}. \quad (25)$$

IV. RESULTS

A. Direct inductive coupling

To be specific, let us first consider the case of circuit A with an inductive coupling, $Z_c = i\omega L$, coupling two identical resistors, $Z_1 = Z_2 = R$, kept at a small temperature difference ΔT . Eq. (11) then provides the expression for the thermal conductance K_L upon substitution of

$$\mathcal{T}_L(x) = \frac{\alpha_L^2}{\alpha_L^2 + x^2}, \quad (26)$$

which is the relevant photon transmission coefficient as a function of the dimensionless frequency $x = \hbar\omega/2k_B T$. The parameter

$$\alpha_L = \frac{\hbar R}{Lk_B T} \quad (27)$$

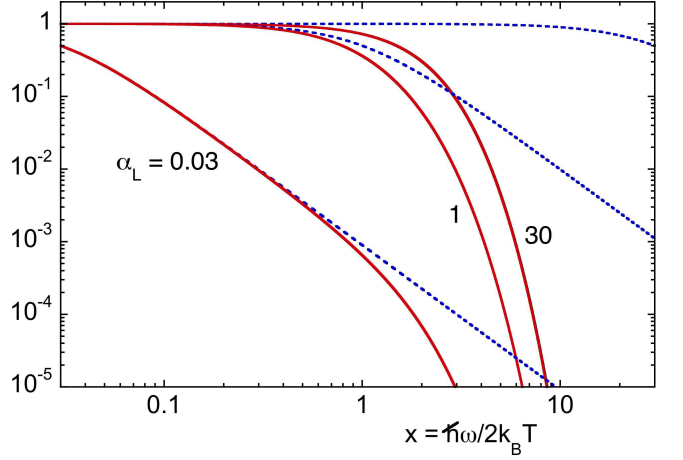


FIG. 2: (Color online) Case of an inductive coupling. Spectrum of the thermal noise power density $x^2/\sinh^2 x$ (black dots), the photon transmission coefficient $\mathcal{T}_L(x) = \alpha_L^2/(\alpha_L^2 + x^2)$ (dotted blue line) and of the product of the two, namely the photonic heat (thin red full line) as a function of the frequency, for values of the parameter $\alpha_L = 0.03, 1$ and 30 from top to bottom. The frequency is plotted in units of the thermal frequency $2k_B T/\hbar$. We consider the case of perfect resistance matching $R_1 = R_2 = R$.

defines the crossover between the low-frequency regime $x \ll \alpha_L$ where the inductance is transparent and the corresponding photon transmission coefficient $\mathcal{T}_L(x)$ is close to 1 and the high-frequency regime $x \gg \alpha_L$ where the inductance becomes opaque and $\mathcal{T}_L(x) \sim \alpha_L^2/x^2 \ll 1$. The result (26) for the photon transmission coefficient can thus be understood as originating from a low-pass LR filter composed of the resistance R and the coupling inductance L that filters the photonic thermal spectrum. The cut-off frequency is given by α_L in units of the thermal frequency $2k_B T/\hbar$, at frequencies beyond the cut-off frequency the transmission decays as $1/x^2$.

We have calculated the spectral density of the photonic heat transferred from one resistor to the other for several values of the parameter α_L . Fig. 2 displays the spectrum of the thermal noise current $x^2/\sinh^2(x)$, the photon transmission coefficient $\mathcal{T}_L(x)$ and of the product of the two. The integral of the latter quantity gives the power transmitted by photons $P_{1,2}$. In the limit $\alpha_L \gg 1$ of a small inductance, i.e. a negligible coupling impedance, the photon transmission coefficient equals to unity over the whole thermal spectrum. The integral is then equal to $\pi^2/6$ and one again recovers the quantum of conductance, $K_L = K_Q$. In the opposite limit $\alpha_L \ll 1$ of a large inductance, the photon transmission coefficient decays when the frequency is increased. The photonic signal is then strongly suppressed: $K_L \ll K_Q$.

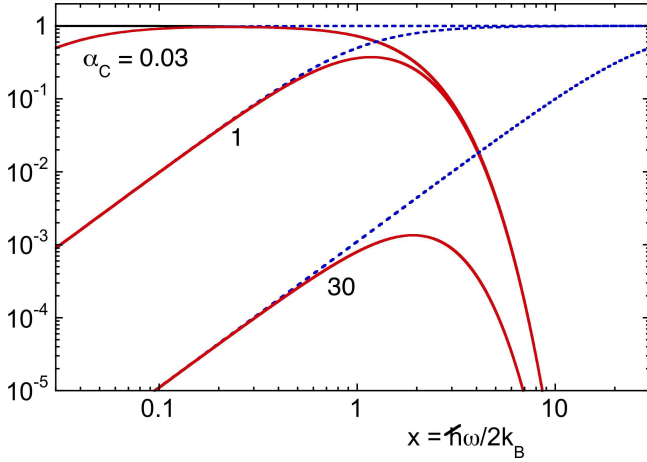


FIG. 3: (Color online) Case of a capacitive coupling. Spectrum of the thermal noise power density $x^2/\sinh^2 x$ (black dots), the photon transmission coefficient $\mathcal{T}_C(x) = x^2/(x^2 + \alpha_C^2)$ (dotted blue line) and of photonic heat (thin red full line) as a function of the frequency, for values of the parameter $\alpha_C = 0.03, 1$ and 30 from top to bottom. The frequency is plotted in units of the thermal frequency $2k_B T/\hbar$. We consider the case of perfect resistance matching $R_1 = R_2 = R$.

B. Direct capacitive coupling

Let us now consider the case of circuit A with a capacitive coupling element $Z_c = 1/i\omega C$. We assume again that the two impedances 1 and 2 are pure resistors with a small temperature difference. The thermal conductance K_C is given by Eq. (11) taking into account the photon transmission coefficient:

$$\mathcal{T}_C(x) = \frac{x^2}{x^2 + \alpha_C^2}. \quad (28)$$

The cross-over frequency is now determined by the parameter

$$\alpha_C = \frac{\hbar}{4RCK_B T}; \quad (29)$$

it separates a low-frequency regime $x \ll \alpha_C$ where the capacitor is opaque and $\mathcal{T}_C(x) \sim x^2/\alpha_C^2 \ll 1$ from a high-frequency regime $x \gg \alpha_C$ where the capacitor is transparent and $\mathcal{T}_C(x) \sim 1$.

Fig. 3 displays information similar to that of Fig. 2 but for the case of a capacitance coupling the two resistors, yielding the photon transmission coefficient \mathcal{T}_C , Eq. (28). The limit $\alpha_C \ll 1$ means that the capacitance is large, i.e. it has a negligible impedance over most of the thermal spectrum. The transparency \mathcal{T}_C is then equal to unity and one recovers $K_C = K_Q$. In the limit $\alpha_C \gg 1$, the photonic signal is strongly suppressed by the RC filter composed of the series capacitance and the receiver resistance, leading to $K_C \ll K_Q$.

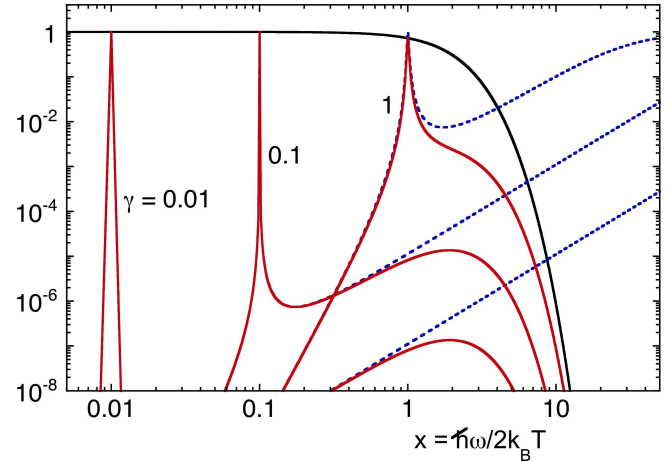


FIG. 4: (Color online) Case of a mutual coupling via an LC-resonator circuit. Spectrum of the thermal noise power density $x^2/\sinh^2 x$ (black dots), the spectral transmission factor $\mathcal{T}_M(x)$ (dotted blue line) and of the photonic heat (thin red full line) as a function of the frequency, for values of the parameter $\gamma = 0.01, 0.1$ and 1 . The frequency is plotted in units of the thermal frequency $2k_B T/\hbar$. We consider the case of perfect resistance matching $R_1 = R_2$ and a parameter $\alpha_M = 30$.

C. Mutual coupling to an LC-resonator

We now turn to circuit B, for the case where the central coupling circuit is an LC-resonator, as indicated in Fig. 1. This means that $Z_c(\omega) = i\omega L + 1/i\omega C$, the resonant frequency is given by $\omega_0 = \sqrt{1/LC}$. Assuming again $R_1 = R_2 = R$ and a small temperature difference ΔT , the thermal conductance K_M is given by Eq. 11 with the photon transmission coefficient:

$$\mathcal{T}_M(x) = \frac{1}{1 + \alpha_M^2(x/\gamma - \gamma/x)^2 x^{-4}}. \quad (30)$$

Here

$$\alpha_M = \frac{R}{2} \sqrt{\frac{C}{L}} \left(\frac{L}{M} \right)^2 \gamma^2 \quad (31)$$

and

$$\gamma = \hbar\omega_0/2k_B T. \quad (32)$$

The photon transmission coefficient is characterized by a resonance at ω_0 , the width of which is governed by the parameter α_M : the larger α_M , the narrower the resonance. For small values of α_M , the transmission coefficient is close to 1 over the thermal spectrum frequency range and we find $K_M \lesssim K_Q$.

D. Coupling through a transmission line

We finally deal with circuit C, with two pure resistors R_1 and R_2 separated by a transmission line that

behaves like a low pass filter with a cut-off frequency $\omega_c = 2/\sqrt{LC}$. In the limit of very low frequency $\omega \ll \omega_c$, the total impedance Z_t is

$$Z_t(x) = (R_1 + R_2) \cos(N\alpha_{TL}x) + i \sin(N\alpha_{TL}x) \sqrt{\frac{L}{C}} \left[1 + R_1 R_2 \frac{C}{L} \right], \quad (33)$$

where

$$\alpha_{TL} = 4k_B T / \hbar \omega_c. \quad (34)$$

For frequencies below ω_c , the impedance Z_t features a series of resonances. At every resonance including the zero-frequency case, the transmission line is fully transparent and the impedance Z_t is equal to $R_1 + R_2$.

At frequencies well above the cut-off frequency $\omega \gg \omega_c$, we can make the approximation $\cos k \simeq -\omega^2 LC/2N^2$. The wave-vector k is then complex. The total impedance is purely imaginary and diverging at high frequency as:

$$Z_t = i\alpha_{TL}x \sqrt{\frac{L}{C}} [-x^2 \alpha_{TL}^2]^{N-1}. \quad (35)$$

From Eq. 7, the transmission coefficient \mathcal{T}_{TL} is related to the line impedance Z_t as: $\mathcal{T}_{TL}(\omega) = 4R_1 R_2 / |Z_t(\omega)|^2$. Fig. 5 shows the transmission coefficient for a number of cells $N = 6$ and $N = \infty$, in the case $R_1 = R_2 = 0.1\sqrt{L/C}$, $\alpha_{TL} = 0.2$. For a finite $N = 6$, we observe a series of resonance peaks, featuring a maximum transmission equal to unity. The case $N = \infty$ corresponds to the continuum limit, where the discretization necessary for the calculation vanishes. In this case, the impedance Z_t is constant and equal to $R_1 + R_2$ over the full bandwidth $[0, \omega_c]$ and infinite above. The transmission is then unity within the bandwidth (if $R_1 = R_2$) and zero above.

E. Total photonic power with reactive coupling

Finally, we have calculated the total photonic power, integrated over the full frequency range, as a function of the parameter α_L or α_C in the respective cases of an inductive or capacitive coupling. We compare both linear and nonlinear response, changing the values of the relative temperature difference $\Delta T/T$, see Fig. 6. In the limit of a small temperature difference and with an inductive coupling, the photonic power decays as α_L when α_L is small. For a capacitive or mutual coupling, the total power is maximal for small $\alpha_{C,M}$; it decays as $1/\alpha_{C,M}^2$ when $\alpha_{C,M}$ is large.

A cross-over between the linear regime $P \propto \Delta T$ and the non-linear regime occurs at $\Delta T/T \approx 1$. When the temperature difference is large, the photonic thermal conductance is larger than the quanta K_Q , because of the broader frequency range of the emitted photons. Only in the case of a significantly inductive coupling $\alpha_L > 1$, which cuts the high frequencies induced by the higher

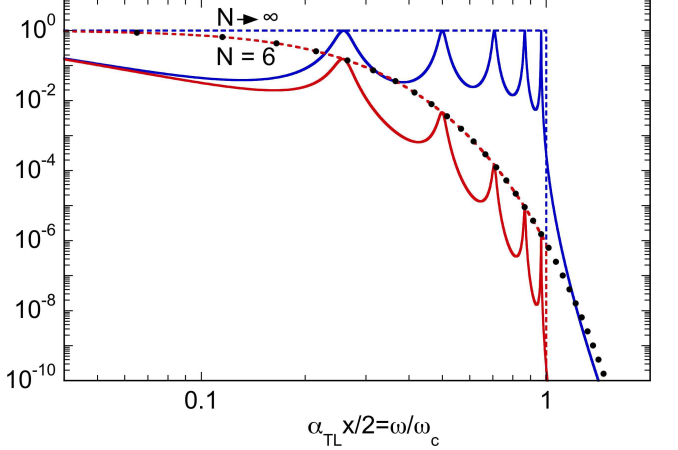


FIG. 5: (Color online) Case of a coupling through a transmission line. Spectrum of the thermal noise power density $x^2/\sinh^2 x$ (black dots), the photon transmission coefficient $\mathcal{T}_{TL}(x)$ (dotted and full blue lines) and of the photonic heat (dotted and full red lines) as a function of the frequency. The full lines stand for a number of cells $N = 6$ and the dotted lines for N infinite. The frequency is plotted in units of the cut-off frequency ω_c . We consider a temperature T so that $\alpha_{TL} = 0.2$ and the case of perfect resistance matching $R_1 = R_2$ with $R = 0.1\sqrt{L/C}$.

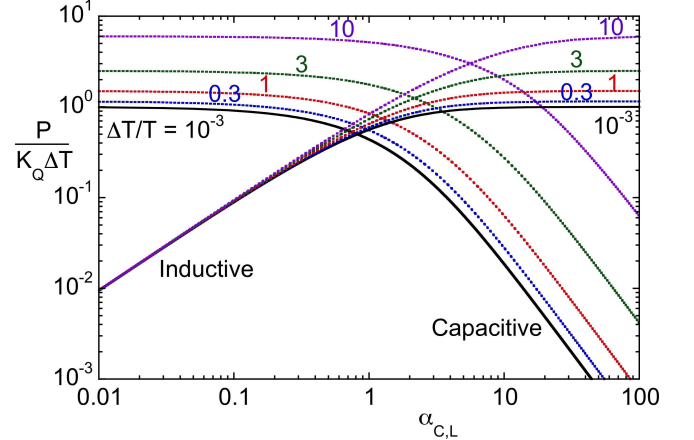


FIG. 6: Dependence of the photonic power through a capacitive or inductive coupling impedance on the parameters α_C or α_L for different values of the relative temperature difference $\Delta T/T$, in units of $K_Q \Delta T$, the maximum photonic power in the case of a linear response.

source temperature, does the thermal conductance not depend on the temperature difference.

In the cases of a coupling through a resonator or a transmission line, the behavior of the total photonic power as a function of the relevant parameter α_M or α_{TL} is similar to the capacitive case.

V. CONCLUSION

In summary, we have introduced a simple circuit approach of the photonic heat transport that can be applied to a variety of experimentally-relevant situations. We would like to stress that this approach operates within a very simple formalism, thus providing an intuitive understanding of photonic thermal conduction channel. This approach enabled us to investigate the phonic heat transfer through a reactive transmission line.

To conclude, let us discuss the possibility to practically use the photonic channel discussed above to transmit power between two electronic circuits that are galvanically isolated. This can be achieved by coupling two resistors through two capacitances. From the above discussion, the maximum efficiency can be attained when the source and receiver impedance are well matched and with a parameter α_C below about 0.1. With impedances of 50Ω , this corresponds to a capacitance value larger than 0.1 pF at a temperature of 4 K or 10 pF at 40 mK , which is significantly higher than the $1\text{-}10 \text{ fF}$ capacitance of typical submicron scale junctions. In Ref. 7, the estimated 10 fF ground capacitance gives a α_C parameter value of about 38 at a temperature of 100 mK . From Fig. 6, one extracts that this results in a heat transfer rate divided by about 1000 compared to the full value, which is consistent with experimental results.⁷ In a real thermal circuit, large series capacitances can easily be integrated using available microfabrication technologies and ensure a fully-efficient photonic channel thermal coupling, while maintaining galvanic insulation. The related thermal conductance is about 1 pW/K at 1 K and scales linearly with the temperature. This approach is thus compatible with the cooling of small objects well decoupled from the thermal bath, like for instance membranes.

As discussed above, photonic heat can also be transmitted through a transmission line, provided that its cut-off frequency is over the thermal spectrum bandwidth. Let us consider for instance a superconducting transmission line made of two strips of width $1 \mu\text{m}$, thickness

50 nm , and separated by $2 \mu\text{m}$. Its kinetic inductance is about 10 pH/mm and its capacitance to the ground about 0.2 fF/mm . The related cut-off frequency is then about 1 K for a length of 10 mm .

Finally, it is interesting to discuss the present results in connection with the "brownian refrigeration" of a cold normal metal in contact with a superconductor via a capacitively shunted tunnel barrier, subjected to the thermal noise generated in a hot resistor¹⁵. For typical system parameters, an optimum exists where a hot resistor of resistance $R = 10R_K$ with $R_K = h/e^2$ gives rise to heat extraction currents of about $10^{-3}\Delta^2/e^2R_T$, where Δ is the superconducting gap and R_T is the tunnel barrier normal-state resistance. However, at the same time, the photon heat channel discussed in the present work will be active, inducing a heat current from the hot resistor *towards* the cold normal metal. This was not included in Ref. 15, where the resistance R_N of the normal metal was set to zero. We can estimate the effect of the photon heat current by modeling the set-up as in A-type circuit: a series combination of the hot and cold resistors of resistance R and R_N , respectively, coupled by a capacitance C . Using typical parameters of Ref. 15 and assuming a resistance mismatch $R_N/R = 0.01$, the direct photon heat current can be estimated to be $10^{-3}\Delta^2/e^2R_K$, which is comparable to or larger than the heat extraction current if $R_T \gtrsim R_K$. In order to recover a net cooling of the cold resistor, it is not possible to reduce R_T below R_K , as spurious higher order tunneling processes in the junction would reduce the heat extraction current. One can however increase the resistance mismatch: the photon heat current is proportional to R_N/R . We conclude that the heat extraction mechanism of Ref. 15 outweighs possible direct photon heating only for metals with resistances R_N of a few Ohms or less.

This work is supported by the Région Rhône-Alpes, the ANR project 'Elec-EPR' and the NanoSciERA project 'Nanofridge'. We thank C. Urbina for raising the question that motivated this work, O.-P. Saira and J. P. Pekola for discussion.

¹ F. Giazotto, T. T. Heikkilä, A. Luukanen, A. M. Savin and J. P. Pekola, Rev. Mod. Phys. **78**, 217 (2006).

² S. Rajauria, P. S. Luo, T. Fournier, F. W. J. Hekking, H. Courtois and B. Pannetier, Phys. Rev. Lett. **99**, 047004, (2007).

³ V. Chandrasekhar, Supercond. Sci. Technol. **22**, 08300 (2009) and references therein.

⁴ J. B. Johnson, Phys. Rev. **32**, 97 (1928); H. Nyquist, Phys. Rev. **32**, 110 (1928).

⁵ D. R. Schmidt, R. J. Schoelkopf, and A. N. Cleland, Phys. Rev. Lett. **93**, 045901 (2004).

⁶ M. Meschke, W. Guichard, and J. P. Pekola, Nature **444**, 187 (2006).

⁷ A. V. Timofeev, M. Helle, M. Meschke, M. Möttönen, and

J. P. Pekola, Phys. Rev. Lett. **102**, 200801 (2009).

⁸ A. V. Timofeev, C. P. Garcia, N. B. Kopnin, A. M. Savin, M. Meschke, F. Giazotto, and J. P. Pekola, Phys. Rev. Lett. **102**, 017003 (2009).

⁹ J. B. Pendry, J. Phys. A **16**, 2161 (1983).

¹⁰ T. Ojanen and A.-P. Jauho, Phys. Rev. Lett. **100**, 155902 (2008).

¹¹ C. W. J. Beenakker, M. Kindermann and Yu. V. Nazarov, Phys. Rev. Lett. **90**, 176802 (2003).

¹² E. M. Lifshitz and L. P. Pitaevskii, *Statistical Physics, Part 2*, Pergamon Press, Oxford (1980).

¹³ U. Sivan and Y. Imry, Phys. Rev. B. **33**, 551 (1986).

¹⁴ D. E. Angelescu, M. C. Cross, and M. L. Roukes, Superlattices and Microstructures **23**, 673 (1998); L. G. C. Rego

and G. Kirczenow, Phys. Rev. Lett. **81**, 232 (1998).
¹⁵ J. P. Pekola and F. W. J. Hekking, Phys. Rev. Lett. **98**, 210604 (2007).